Tanker Q&As and CIs on the IACS CSR Knowledge Centre

KCID No.	Ref.	Type	Topic	Date completed	Question/CI	Answer	Attachment
85	App. C/1.4.4.11	Question	fatigue calculation	2006/10/5	Span of Longitudinal in fatigue calculation:The span of longitudinals i.w.o. the bilge may be reduced when they are supported by bilge brackets.	The decision whether the bilge bracket provides support depends on the actual depth, length and scantlings of the bilge bracket itself. A review will have to be made in each instance depending on the actual offered arrangements.	
138	App. C, Table C1.7 Note (1)	Question	Attachment length	2006/9/11	150mm should include (ignore) the size of scallop? 2. If flat bar size is 150mm but its soft toe is 200mm, the “one grade up” does not apply?	Attachment length is defined as “length of the weld attachment on the longitudinal stiffener face plate without deduction of scallop”. 2. The attachment length is larger than 150 mm, therefore it cannot be upgraded.	
139	App. C, Table C1.7 Note (6) (7)	Question	Range of Dynamic Wave Zone	2006/9/27	What is the range of Dynamic Wave Zone in Inner hull? Center L.BHD and Double bottom girder included in Dynamic Wave Wetted Zone?	The words "Dynamic wave wetted zone" only apply to the "at side" part of the sentence. It means Note 6 applies to "dynamic wave wetted zone at side" AND "in way of bottom" and "in way of inner hull below 0.1D from deck at side". Section 9/3.3.1 and Appendix C/Table C.1.5 do not cover double bottom girders. Therefore, fatigue assessment is not required for double bottom girders. Note 6 in Table C.1.7 does not apply to inner longitudinal bulkheads. Note 7 in Table C.1.7 applies to inner longitudinal bulkheads.	
140	App. C, Table C1.7 Note (6) (7)	Question	Definition of "conventional slot"	2006/10/24	Does the conventional slot configuration include collar plate? What is the definition of “conventional slot”? Is it affected by collar plate?	1. “conventional slot” refers to the shape of the opening for the stiffener. Examples are shown in Figure 6.5.9 for example. 2. Collar plate is required for the cases 1 and 4 in Figure C.1.11 in the application of Note 6 in Table C.1.7. Please note that, in case the collar plate is welded to the face of the flange, then ID31 and Note 5 apply.	
141	App. C, Table C1.7 Note (7)	Question	Class for conventional slot	2006/9/27	Class F should apply for “conventional slot”. In this case, if “tight collar” is fitted, can class E apply?	Class F should apply in general for "conventional slot" unless alternative condition in Corrigenda 2 is satisfied. In case tight collars are fitted on deck and within 0.1D below deck at side, Note (5) applies instead of Notes (6) and (7). This means that Class F should be also applied for connections with tight collars in this region.	

KCID No.	Ref.	Type	Topic	Date completed	Question/CI	Answer	Attachment
153	2/3.1.8.2, App C/1.3.2	Question	Cargo mean density used for simplified fatigue calculations	2006/10/9	The treatments of the cargo mean density used for the simplified Fatigue Calculation in Appendix C: Are the cargo mean density used 0.9 specified in Sec.2/3.1.8.2 or the density corresponding to the loading condition at the scantling draught in full load homogeneous loading condition under the condition of approval of the Class? If the design specification of ships gives the cargo density corresponding to the alternate loading condition, which is regarded as the option contracted by shipbuilder and ship owner, can the classification society be disregarded such option under the approval of such design?	1. The cargo density of 0.9 tonnes/m3 or the cargo density of homogeneous scantling draught, whichever is greater, is to be used. 2. As specified in Section 2/3.1.10.1.(g), higher cargo density for fatigue evaluation for ships intended to carry high density cargo in part load conditions on a regular basis is an owner's extra. Such owner's extra is not covered by the Rules, and need not be considered when evaluating fatigue strength unless specified in the design documentation.	
155 attc	C/1.4.5.14	Question	Weld Connection	2006/10/5	On the premise that the requirement of 1.4.5.14 is limited to apply to weld connection between the hopper plate and inner bottom, is the example shown the figure below acceptable as the improvement measure for fatigue strength complying with the requirement?	Proposal considered satisfactory in relations to the stipulated rule requirement in case where fatigue life improvement is desired as per Appendix C 1.4.5.14. The grinding requirement could be based on International Institute of Welding (IIW) Recommendations.	Y
156 attc	Figure C.2.2	Question	Dressed & Ground smooth	2006/11/6	(1) It is requested to clarify the "dressed" and "ground smooth" which are stated in Figure C2.2 of Appendix C and to specify in the detailed procedure of such improvement measure. (2) In the Figure C2.2 of Appendix C, extent of dressing both side of floor. VLCC: 250mm, Suezmax: 200mm, Aframax: 150mm, Product: 100mm Is value able to be applied to grinding of the weld toe, too? (3) We would like to know the reasons why the recommended value of the extent of dressing is different corresponding to the vessel size. It is seemed to be little difference the structural arrangement of such hopper parts regardless the ship size.	1)Dressing to read as bead dressing i.e. as per attached figure. "Grinding smooth" means smooth concave profile and small weld flank angle. The rules need update to clarify this. 2)That is correct, extent of "grinding smooth" is the same as the extent of dressing 3) We will consider future update of the rules e.g. apply one limit of 200mm for all size of tankers.	Y
158	App C/2.1.1.2	Question	Bilge knuckle of bent type	2006/10/9	Where the bilge knuckle is the bent type, is it not necessary to carry out the fatigue check to such type because the standard structural details and minimum requirement to such part are given in Figure C.2.4?	The Rule Appendix C/2.1.1.2 reads: "When alternative design is proposed, a suitable finite element (FE) analysis should be used to demonstrate the equivalency of the detail in terms of fatigue strength." As a minimum, a comparative hotspot stress analysis should be carried out, using the recommended design as benchmark.	

KCID No.	Ref.	Type	Topic	Date completed	Question/CI	Answer	Attachment
175	App. C, Table C1.7 Notes (1) & (2)	CI	Selection of SN curves for fatigue details	2006/10/9	Regarding the selection of SN curves for fatigue details given in CSR Rules Tab. C.1.7, the notes at the beginning are confusing since we are in both situations of notes 1 & 2. For example, if we have bulb stiffeners with flat bars at ends less than or equal to 150mm. In one case we can upgrade the SN-curve and in the other one, we have to downgrade and so we assume finally that we use the same curve without taking account of the Notes 1 & 2. Could you please confirm if it is correct?	You are correct. As such, if there is a bulb stiffener and the clearance between the edge of the stiffener flange and the face of the attachment (in this case is a flat bar) is less than 8 mm, the fatigue class needs to be downgraded. If the attachment length of the flatbar is less than 150mm, the fatigue class needs to be upgraded. Then, it goes back to the fatigue class specified in the Table C.1.7.	
281	C/1.4.1.3	Question	fatigue assessment	2006/11/13	The fatigue calculation is based on homogeneous full load and normal ballast conditions with a proportion of ship's life of .5 each. This may be realistic for a pure oil tanker. But in case of product tanker the loading conditions are different. Here we will not have the strict regime of one journey in full load condition is followed by a journey in ballast condition. The CSR for Bulkers offer an approach which is dependent of the ship's size, based on the assumption that smaller ships operate in a different trade. How can this be handled within CSR for Tankers?	The voyage assumptions for fatigue calculation are the same for crude oil tankers and product oil tankers.	
310	Fig C.2.2	Question	kuckle connection	2006/12/19	We have been informed that IACS are discussing / have decided to increase the building tolerance for the lower knuckle connection from 0.15 t to t/3 with a maximum of 5 mm. Will appreciate if you could discuss in detail the effect that the subject change will have on stresses / fatigue life for a connection designed as per CSR for a typical Aframax, Suezmax and VLCC hopper. Our understanding is that no thickness or welding improvements have been proposed to counterbalance whatever negative effect the increased tolerance will have.	This change of the building tolerance was made in RC Notice No.1 adopted in Sept '06 and will effect on 01/04/2007. This change is a correction of irrelevant tolerance, i.e., the previously cited 0.15t was related to the alignment of face plates of primary support members and was not applicable to the alignment of the hopper area. Since this change is a correction of irrelevant tolerance, no thickness or welding improvements to counterbalance this change is applicable.For the welded knuckle between inner bottom and hopper plate, fatigue analysis using a FE based hot spot stress analysis is carried out. Hot spot stresses are to be calculated using an idealized welded joint with no misalignment since the FE model is made with thin shell elements. Since the actual structure in way of this connection has substantial plate thickness, certain building tolerance may be accepted provided it is within certain established limits. The revised building tolerance is still more stringent than the building tolerance in accordance with IACS Recommendation No.47 "SARQS", which is generally applied for the existing Rules.	

KCID No.	Ref.	Type	Topic	Date completed	Question/CI	Answer	Attachment
396	C/2.4.2.7	Question	Fatigue Stress Assessment	2007/6/13	We carried out a fatigue strength assessment on a lower hopper knuckle of VLCC in accordance with CSR. In the assessment, we intended to increase the cargo density from 0.9t/m^3 specified as a minimum one. We generally understood that higher cargo density or accelerations acting on cargo tanks decrease fatigue life of the lower hopper knuckle. However, we obtained longer fatigue life by increasing the cargo density. It differs from our understanding and knowledge. The cause is in the combination formula prescribed in App.C.2.4.2.7: S=f_model|0.85(S_e1 + 0.25S_e2) - 0.3S_i| for full load condition, where S_e=stress range caused by external pressures; and S_i = stress range caused by internal pressures. We would like to ask you to reconsider the formula technically.	In general, the stress range caused by dynamic external pressure is higher in way of hopper knuckle than that caused by internal pressure. The formulation in Appendix C2.4.2.7 has been derived based on this premise and calibrated with a cargo density of 0.9t/m3. Also considering that the actual cargo densities used in the ordinary oil tanker operation are even smaller than the specified maximum cargo density as per Section 2/3.1.8.2, it is our intention to limit the cargo density to 0.9t/m3 only for fatigue assessment of hopper knuckle connection even if a higher cargo density is used for fatigue assessment of ordinary longitudinal stiffener end connections. Consequently, cargo density of 0.9t/m3 is to be always used for fatigue assessment of hopper knuckle connection. We will update the applicable rule text to clarify this.	
412 attc	C/1.4.5.12	Question	Thickness Effect	2007/3/30	There were some doscissopms pm tjoclmess effect fp the 2nd draft. And the final reply from JTP was that it would be retained in the JTP Rules. With this regard, Yagi et al. [Ref.1 and 2] conducted comprehensive parametric experiments to revela thickness effect with thinkness ranging from 10mm to 80mm. In these papers, it is concluded that the as-welded joints with constant sized attachemnts in tension have a thickness effect exponent of - 1/10 compared to the rule value (-1/4) based on DEn and IIW fatigue guidelines, while as-welded joints under bending stress have severer thickness effect o f an exponent of -1/3. It was also found out that the thickness effect becomes much milder if the weld profile is improved by grinding. We would appreciate it if these items will be further studied for furture improvement of the CSR. Reference document: Ref. [1] J.Yagi, S.Machida, Y. Tomita, M.Matoba, I.Soya: influencing Factors on Thickness Effect of Fatigue Strength in As-Welded joints for steel structures, journal of SNAJ Vol.169 (1991) (in Japanese); Ref.[2] J.Yagi, S.Machida, Y.Tomita, M.Matoba, I.Soya: Thickness effect criterion for fatigue evaluationof welded steel structures, journal of SNAJVol.169 (1991) (in Japanese)	The power index for stress concentration factor due to thickness effect is based on DEn recommendation of -0.25. DEn recommended S-N curves also used in the Common Structural Rules. For small attachments only, e.g. web stiffener connection to face plate of longitudinal stiffener, a different index is used by some design codes (which produces a less conservative result than using index of -0.25) and this may be considered in future rule improvement. For assessment of hopper knuckle connection (cruciform joint, see CSR Appendix C, 2.4.3), it is considered that a power index of -0.25 is appropriate. Grinding can reduce effect due to thickness, however, the power index is in an order of not less than -0.2 in general, hence we consider that the power index of -0.25 is still appropriate considering that the variation in workmanship and CSR also allows a separate improvement factor for ginding.	Y
509	C/2.4.2.6	Question	Obtaining stress by linear interpolation or other interpolation methods	2007/9/5	The Rule shows that the stress may be obtained by linear interpolation or other interpolation methods. The problem is that stresses obtained by different interpolation methods are different evidently. For example, the stress obtained by Lagrange method is less than one by linear interpolation. So the results of the fatigue assessment are quite different. The interpolation method is proposed to be clarified in the Rule.	The fatigue method has been calibrated on a linear interpolation between elements. Consequently the interpolation method to be used is the linear one between the centres of gravity of the 1st and 2nd elements from the structure intersection.	

KCID No.	Ref.	Type	Topic	Date completed	Question/CI	Answer	Attachment
531	C/1.4.4.11	Question	stress factor in simplified fatigue strength calculation	2007/10/2	The stress factor in simplified fatigue strength calculation. The subject Rules say "Kd factor may be determined by FE analysis of the cargo hold model where the actual relative deformation is taken into account". In this case, which loading conditions should be considered ? Although simplified fatigue assessment just consider normal ballast condition & homo loading condition, there is no ballast loading conditions in FE loading cases except for emergency ballast loading condition which we think it is not appropriate to be considered.	IACS have no common procedure for determination of Kd by FE analysis this need to be particularly considered by each class society.	
575 attc	7/4, 8/2, App.B & App.C	CI	Tank approval procedure for cargo tanks	2008/3/28	Please clarify CSR tank approval procedure for cargo tanks design for carriage of high density cargo with partial filling and restriction on max filling height.	Please see attached file: 2.9 - (CIP) Common Interpretations April 2008	Y
605	C/1.4.4.11	Question	Wash Bulkheads in wing cargo tanks	2007/11/16	On VLCCs having wash bulkheads in wing cargo tanks but no wash bulkheads in center cargo tank at the same section, presume that Kd factor for typical frame location may be used for the location in center cargo tanks, which is the same secton as wash bulkheads in wing cargo tanks. As such,the Kd factors required for transverse/wash bulkhead connections need not be applied for such location in center cargo tank where no wash bulkhead actually exists. Please confirm.	The arrangement described with wash bulkhead in Wing Tanks is the most common structural arrangement for VLCC and Kd=1.15 apply to all longitudinals without exception.	

KCID No.	Ref.	Type	Topic	Date completed	Question/CI	Answer	Attachment
642	C/1.4.4.19	Question	Corrosive correction factor (fSN)	2008/2/13	We would like to know if the corrosive correction factor (fSN) used in the nominal stress approach (App. C, 1.4.4.19) may be used in the hot spot stress (FE Based) approach (appendix C.2 of CSR for Oil Tankers). The coefficient (fSN) is not mentioned in Appendix C/2.4.3.1.	fSN is not included in the formula given in C/2.4.2.7 and does not apply to hot spot stress fatigue calculation for hopper corner.	
643	C/1.4.5.14	Question	Application of grinding effect	2008/2/4	Please, could you provide us technical background of the 17 years required for the application of grinding effect (Appendix C, 1.4.5.14 in CSR Oil Tankers).	We have included a minimum requirement of 17 years that the structural detail and scantlings have to satisfy without resorting to grinding (application of a factor of two). If we did not have a minimum indicated then designers could apply grinding right from the start, which if used, would end up with details with a fatigue life of 12.5 years without resorting to grinding. The original fatigue codes indicate that the grinding (weld improvement) should not be used in design, but instead used to improve the detail later in-service or to apply an added level of safety. In other words the codes realize that weld improvement improves the life, but would rather it not be used in design. Therefore the IACS CSR developers, we, were left with the choice of not allowing the use of grinding at all in accordance with the original codes, or, to fully allowing it. At first we decided to fully allow it, but a few Technical Committee members did not agree and rather than totally not allowing it they commented that grinding could be "partially used" for the last 20 to 25 percent of the required 25 year life. We arrived at 17 years because it is an integer,so we rounded down to 17 years rather than up to 18 years. There is no scientific proof or experimental test data to prove one way or the other regarding the use of 17 years as the minimum to obtain prior to resorting to grinding.We did not relay on any tests that we were obtained from shipyard.	
814	C/2.4.2.6	Question	hotspot stres	2008/9/29	Does the Rule calls for extrapolation to the floor position for the determination of hotspot stress iwo hopper knuckle.	We can confirm that the extrapolation is only to be carried out in the transverse direction.	

KCID No.	Ref.	Type	Topic	Date completed	Question/CI	Answer	Attachment
828	C/1.4.4.6	CI	openings	2008/9/24	With regard to the rule wording "(openings deducted)" in Appendix C/1.4.4.6 and 1.4.4.8, presume that this "opening" is "Large openings and small openings that are not isolated" indicated in 4/2.6.3.4 provided that the conditions for "isolated small openings" in 4/2.6.3.7 are met. As such, isolated small openings need not be deducted for fatigue analysis provided that the conditions in 4/2.6.3.7 are met. Please confirm."	Your interpretation is confirmed; to avoid any confusion "(openings deducted)" will be deleted from C/1.4.4.6 and C/1.4.4.8 at the next Rule change.	
934	Text C/1.4.5.12	CI	reference thickness	2009/7/3	In this paragraph there is a reference to a "reference thickness of 22mm". It is not clear whether this is a net or gross thickness.	The "reference thickness of 22mm" is a net thickness.	
981 attc	Table C.1.7	Question	fatigue assessment	2009/10/23	Note 6 in Table C.1.7 says "Equivalence to Figure C.1.11 is to be demonstrated through a satisfactory fatigue assessment by using comparative FEM based hot spot stress of the cut-out in the primary support member and the collar". Our understanding is that different slot configurations may be accepted if the hot spot stress of the actual structure which leads to fatigue strength is verified as equivalent with that of rule required scantling and slot configuration. For example, Due to the shape of higher stress concentrations, we understand that straight touched web/collar plates normally can't be accepted as alternatives to soft toe types. However, as shown in the attachment, if the web/collar plate thickness is additionally increased to compensate for any stress concentrations, the hot spot stress of Type B designs can be reduced to the equivalent level of Type A even if the straight touch is applied. Considering the above, we understand that such kind of alternative (Type B) can be accepted subject to: (1) Shear stress of connections under the requirements of CSR Section 4.3.4 having enough of a safety margin to compensate for any stress concentrations by different slot shapes. (2) The stress concentration factor is well verified by FEM assessment with hot spot stress approach. Please confirm that our above understanding is correct.	Equivalence to Figure C.1.11 is to be demonstrated through a satisfactory fatigue assessment by using comparative FEM based hot spot stress of the cutout in the primary support member and the collar. Your item 1): It is not sufficient to investigate only the local shear stress of the connection. A connection can have sufficient shear capacity but high stress concentration can still be present at the opening corner to the LSM. Your item 2): Local shear, PSM shear and bending stress components has to be taken into account. We intend to make a common interpretation to have a common procedure describing how to carry out the comparative FEM study.	Y

KCID No.	Ref.	Type	Topic	Date completed	Question/CI	Answer	Attachment
989 attc	App C 1.5, Table C.1.7 Note 1	CI	Attachment length	2010/8/12	Where the attachment length is less than or equal to 150mm, the S-N curve may be upgraded one class from those specified in the table. For example, if the class shown in the table is F2, upgrade to F. Attachment length is defined as the length of the weld attachment on the longitudinal stiffener face plate without deduction of scallop. But this will cause unexpected results (See attachment) which are difficult to explain why soft toe bracket has less fatigue life than flat bar. In this regard "Attached length" should be replaced with "The depth of stiffener". (See attachment)	The harmonisation project is currently ongoing and is considering the fatigue requirements of the two CSR Rules. You proposal will be retained and included in the project.	Y
996 attc	Table C.1.7 & Fig 4.1.4	CI	Cut-outs in lower stool	2010/3/8	We understand that normal cut-out type for the cloud mark area in the attachment is not acceptable if web stiffener is omitted as described in note 6 of Table C.1.7. However, KC 139 is not clear defining inner longitudinal bulkheads as quoted below; Quote "Note 6 in Table C.1.7 does not apply to inner longitudinal bulkheads" Unquote Our understanding is that inner longitudinal bulkhead in the above means the longitudinal bulkhead as shown in Fig. 4.1.4 and considering the inner hull definition in Table 4.1.1 & MARPOL req't, Note 6 in Table C.1.7 is also applicable to the cloud mark area since the concerned area is boundary between cargo and ballast tank. Please confirm.	In Note 6 of Fig.C.1.7, optimized slots are required in way of flat-barless connections for the inner bottom and hopper, but not the centerline bulkhead. It could be argued that the stool is categorized as part of the longitudinal bulkhead. But considering that the stool is open to the double bottom ballast tank we would categorise it as being part of the inner bottom. The lateral pressure in way of the stool is expected to be close to that on the hopper or inner bottom. Ordinary slots may be permitted if satisfactory fatigue life is demonstrated.	Y

KCID No.	Ref.	Type	Topic	Date completed	Question/CI	Answer	Attachment
1021 attc	Table C1.3, C1.4, C1.5	Question	Value of stress range combination factor f2 corresponding to stress range due to Horizontal BM	2010/5/27	Regarding the stress combination factors (f1, f2, f3 and f4) specified in Table C.1.3 to C.1.5, we consider that the f2 values, the stress range combination factor corresponding to stress range due to horizontal bending moment, under normal ballast conditions are unreasonable for the following reasons: (See attached) 1.The “f2” value of the upper part of the inner hull is about twice as much as that of the upper deck. 2.The “f2”value of the upper part of the inner hull is greater than twice that of the upper part of the side shell. From our studies, we have found that the fatigue assessment of an uppermost longitudinal stiffener fitted on an inner hull (IL1) is more severe than that of an uppermost one fitted on a side shell (SL1) due to f2 value differences under normal ballast conditions. We think that the f2 values for these longitudinals should be almost the same under normal ballast conditions. The CSR technical background regarding the stress combination factors is as follows: (a)Stress range combination factors are derived based on the theory of a stationary ergodic narrow-banded Gaussian process. (b)The total combined stress in short-term sea states is expressed by linear summation of the component stresses with the corresponding combination factors. This expression is proven to be mathematically exact when applied to a single random sea. (c)The long-term total stress is similarly expressed by linear summation of component stresses with appropriate combination factors. Could you kindly give us the detailed technical background on the determination of the stress combination factors? Your prompt reply would be greatly appreciated.	As the contributing stress range components Sv, Sh, Se and Si and total stress range for the inner hull and the side shell are not expected to be identical, the combination factor for stress due to horizontal bending moment, f2, for the inner hull and the side shell is also expected to be different. For theoretical background of the stress combination approach, please see attached paper. We have not so far encountered similar feedback from designers applying the rules; however your feedback is appreciated. We would be able to make further investigations if design information for the ship concerned with calculation inputs and results are provided.	Y
1038 attc	C/2.2.1.1	CI	Calculation of average net thickness and material for FE yield & buckling evaluation	2010/6/25	For FE when the different thickness and material is used within one panel between stiffeners, the average net thickness (See detail in the attached figure 1) and the lowest material to be used for yield and buckling evaluation. Please confirm.	For FE when the different thickness and material is used within one panel between stiffeners, the average net thickness and the lowest material to be used for yield and buckling evaluation as proposed.	Y

KCID No.	Ref.	Type	Topic	Date completed	Question/CI	Answer	Attachment
1097	Text 9/2.3.1, App.B/3.1, Sec.9/3.3, App.C/2	Question	Fine mesh analysis on hopper knuckle connection	2011/10/5	Upper hopper knuckle connections are required to be evaluated by fine mesh analysis according to Section 9/2.3.1 and Appendix B/3.1. While lower hopper knuckle connections are required to be by very fine mesh fatigue analysis according to Section9/3.3 and Appendix C/2. We consider that structural assessment of upper hopper knuckle connections similar to lower hopper knuckle connections is possible to be carried out by very fine mesh fatigue analysis that is more advanced calculation than fine mesh analysis. Is it acceptable that very fine mesh fatigue analysis for structural assessment of upper hopper knuckle is carried out?	There is currently no procedure (in CSR OT) to carry out a fatigue assessment of the upper hopper knuckle and individual class requirements should be followed.	

KC#155

Weld connection between the hopper plate and inner bottom

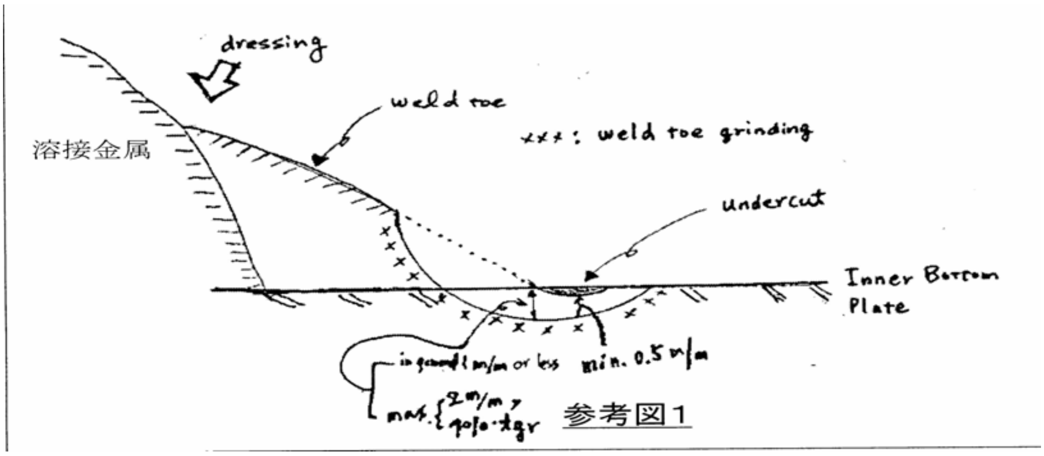

参考図1

KC#156

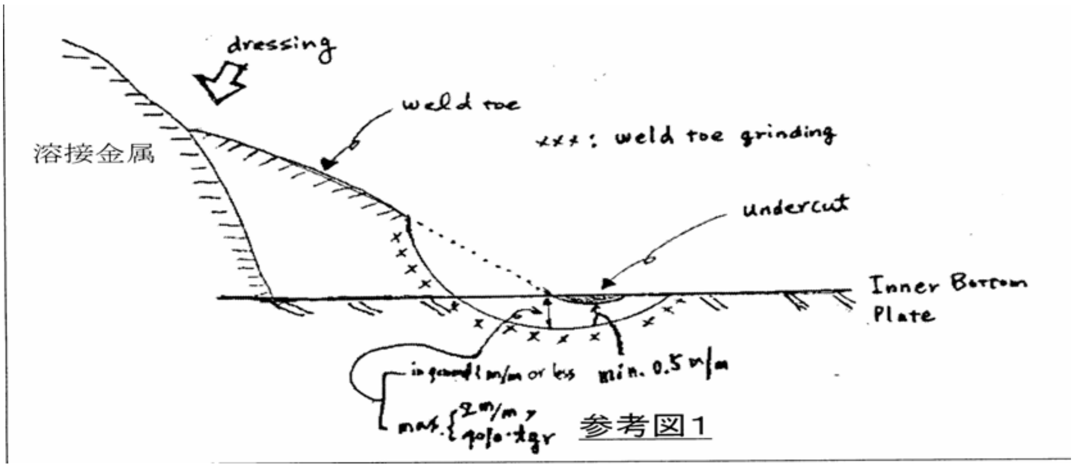
dressing
weld toe
xxx : weld toe grinding
溶接金属
undercut
Inner Bottom
Plate
min. 0.5 m/m

参考図1

KC#412

溶接継手の疲労強度に関する板厚効果評価基準の検討

正員 八木順吉* 正員 町田 進**
正員 冨田康光*** 正員 的場正明**
正員 征矢勇夫****

Thickness Effect Criterion for Fatigue Evaluation of Welded Steel Structures

by Junkichi Yagi, *Member* Susumu Machida, *Member*
Yasumitsu Tomita, *Member* Masaaki Matoba, *Member*
Isao Soya, *Member*

Summary

In this study, the thickness effect was investigated by systematic experiments on welded steel joints with thicknesses ranging from 10 to 80mm. Cruciform joints and Tee joints with improved weld by overall profiling or toe-grinding were tested under pulsating tension and under pulsating bending, respectively.

These experimental results were analyzed together with the previous results of as-welded joints. As a result, it was concluded that the thickness effect exponents for various conditions may be classified into three categories according to the combination of joint type and loading mode. As-welded joints under bending stress have the greatest thickness effect exponent of $-1/3$, while as-welded joints under tension having an exponent of $-1/5$. If the weld profile is improved by grinding, the thickness effect becomes much milder to an exponent of $-1/10$. The as-welded joints with constant-sized attachments also have an exponent of $-1/10$. Furthermore, thickness effect dependency on fatigue life was investigated.

Based on these results, a new evaluation criterion for design purposes has been proposed in this study.

Test Specimen

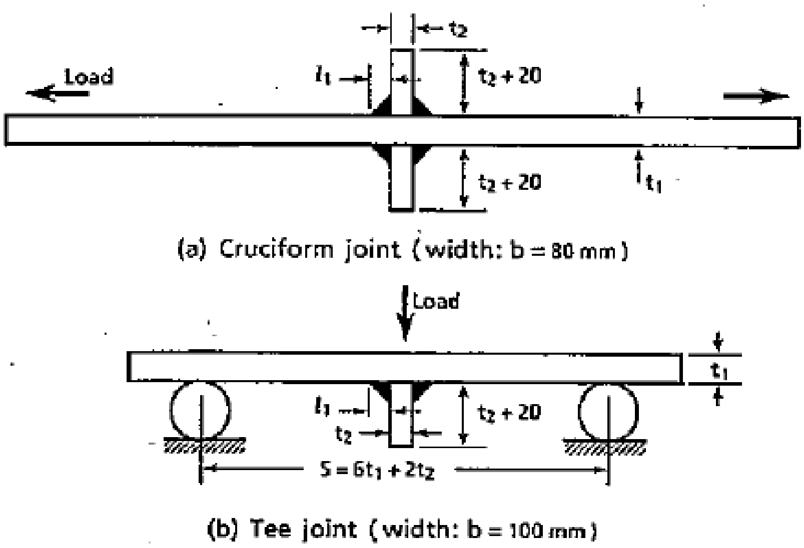

Fig. 1 Tensile and bending fatigue test specimens

Table 1 Fatigue test series of improved joints

Loading	Welded Attachment	Weld Treatment	Code of Series	Main Plate Thickness, t_1 (mm)
Tension	Proportional	Profile	PC1	10, 22, 40, 80
	Constant	Profile	PC2	22, 40, 80
	Proportional	Grinding	GC1	10, 22, 40, 80
Bending	Proportional	Profile	PT1	22, 40, 80
	Constant	Profile	PT2	22, 40, 80
	Proportional	Grinding	GT1	22, 40, 80

Table 2 Dimensions of improved welds

Type of Joint	Main Plate Thickness t_1 (mm)	Rib Plate Thickness t_2 (mm)	Weld Leg Length (mm)		Grinding of Weld Toe	
			l_1	l_2	p (mm)	θ (°)
Proportional Joint	10	5	4	4	1.5	40
	22	10	9	9	3	40
	40	22	16	16	6	40
	80	40	32	16	6	25
Constant Joint	22	22	16	16	6	40
	40	22	16	16	6	40
	80	22	16	16	6	40

Summary results of exponents of thickness effect obtained from the experiments
(Dotted line is drawn at -m=0.25 in accordance with UK DEn)

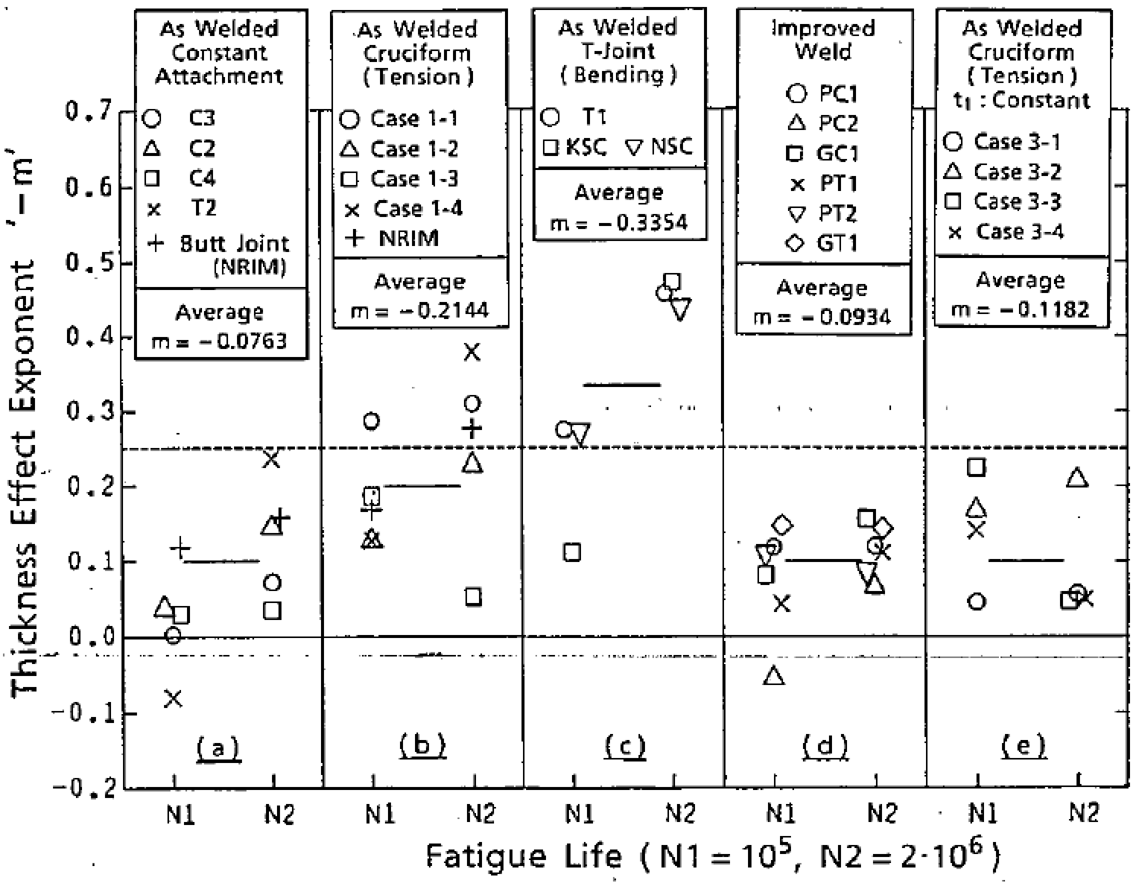

Fig. 13 Thickness effect exponents in various kinds of joints

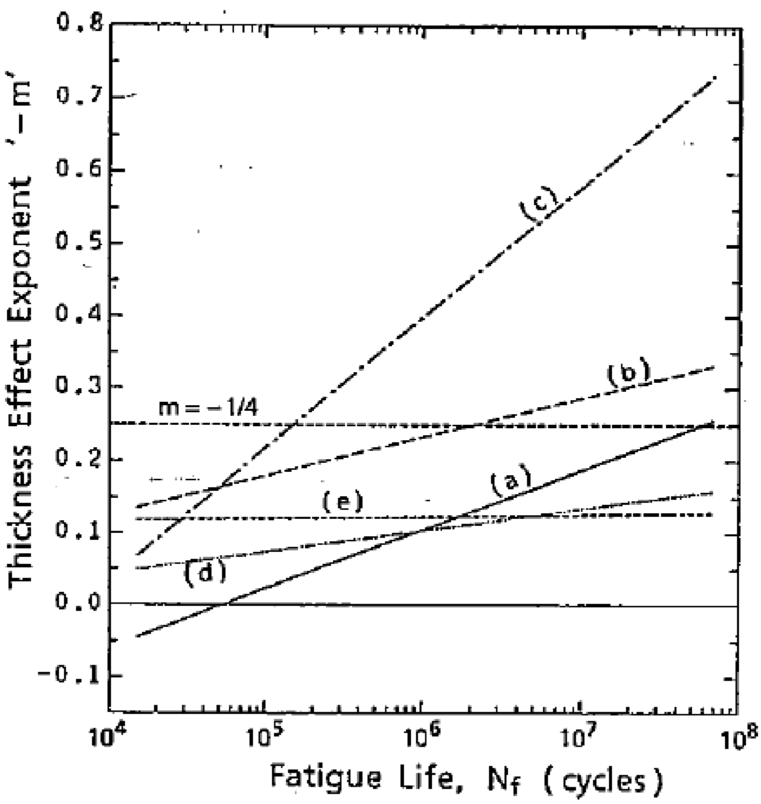

Suggested exponents of thickness effect based on the experiments

Table 3 Joint category associated with thickness effect exponent

Joint Category	Thickness Effect Exponent
(A) As-welded joint in which bending stress is dominant and its basic design S-N curve has been obtained by bending fatigue test.	$m = -1/3$
(B) As-welded joint in which tensile stress is dominant, or as-welded joint for which, even if bending stress is dominant, basic design S-N curve has been obtained by tensile fatigue test.	$m = -1/5$
(C) 1. As-welded butt joint. 2. As-welded joint with welded attachment smaller than a certain size. 3. When joint which is categorized at $m = -1/3$ or $-1/5$ is improved by grinding.	$m = -1/10$

CI-T 2
(Mar. 2008)

Approval of high density cargo limitation on max filling height

Rule Section

7/4	Sloshing and impact loads
8/2	Cargo Tank Region
App. B	Structural Strength Assessment
App. C	Fatigue Strength Assessment

Description

What calculation procedure applies for approval of high density cargo with restriction on max filling height?

Common Procedure

Filling height of high density liquid cargo, h_{HL}, is not to exceed the following:

$$h_{HL} = h_{tk}\left(\frac{\rho_{appd}}{\rho_{HL}}\right)$$

where,

h_{tk}: tank height
ρ_{appd}: maximum density approved for full filling
ρ_{HL}: density of intended high density cargo

LSM/PSM pres. requirements (Sec.8/2)
no additional checks (assuming ρ_{HL} results in bottom pressures equal to that resulting from density of sea water)

Sloshing(7/4)
- Density of intended high density cargo at maximum filling height and below to be used
- If multiple densities of heavy cargo are intended, it may be necessary to assess sloshing with multiple densities with each corresponding maximum filling height.

Fatigue assessment
Sec.2/3.1.8.2 cargo density of homogeneous fulload condition at full load design draught, T_{full}, minimum 0.9tonnes/m^3.
The cargo density of 0.9 tonnes/m^3 or the cargo density of homogeneous full load design draught, T_{full}, whichever is greater, is to be used. 2. As specified in Section 2/3.1.10.1.(g), higher cargo density for fatigue evaluation for ships intended to carry high density cargo in part load conditions on a regular basis is an owner's extra. Such owner's extra is not covered by the Rules, and need not be considered when evaluating fatigue strength unless specified in the design documentation.

FE assessment
Additional load cases for reduced filling height of a tank are to be based on the standard load cases (full tank) with the density modified as:
$\rho_{appd} = \rho_{HL}$ x (h_{HL} / h_{tk})

Loading Manual
Maximum permissible filling height of high density liquid cargo is to be indicated in the loading manual.

Implementation date

This CI is effective from 1 April 2008.

Background

LSM/PSM pres. requirements (Sec.8/2):
Based on density of sea water, which gives same pressures (within a small margin) as that of reduced filling, hence no additional calculations necessary

Sloshing
HL filling will give increased sloshing pressures, hence need to be checked

Fatigue assessment
Requirement is given in Sec.2/3.1.8.2. Is normally based on cargo density from loading manual, however it is shown that increased density have no effect on fatigue life (dominated by ballast condition below NA) except from uppermost stiffeners in cargo tank, which will not be subject to pressure due to reduced filling.

FE assessment
The principle in CSR is that there are predefined load cases and additional load cases need to be added if the loading manual shows more severe conditions than that assumed in the CSR load cases.

KC#981

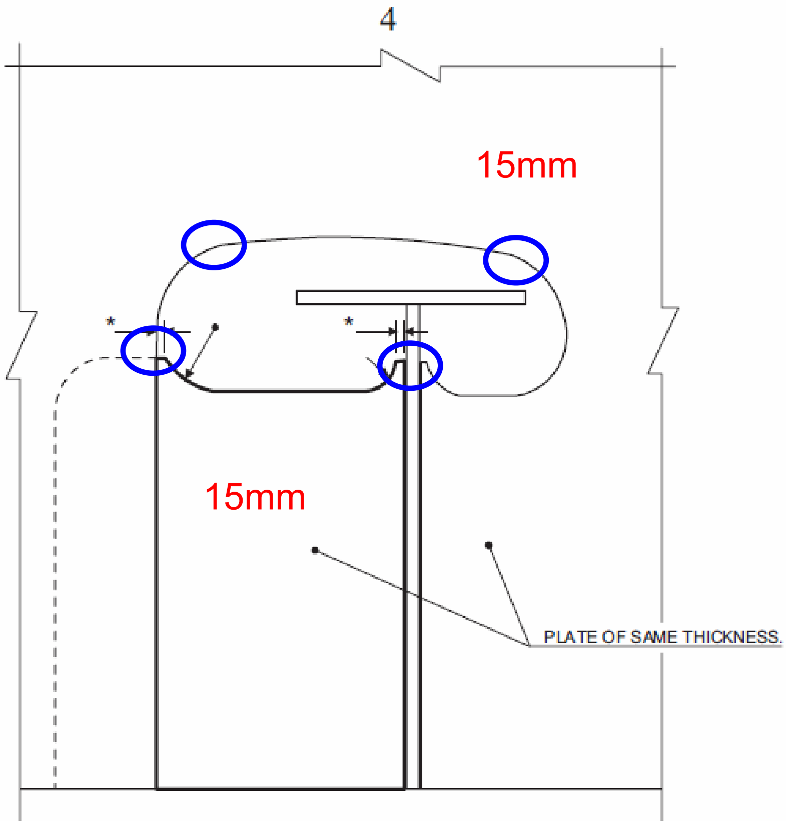

Type A : Fig.C.1.11

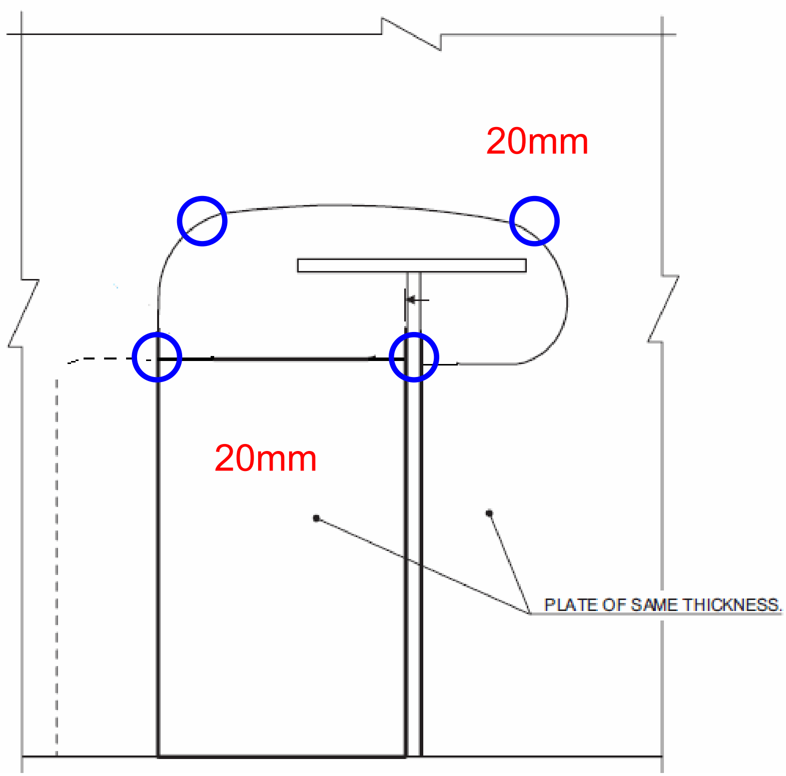

Type B: Alternative

<u>If the hot spot stress is equivalent by the increased web/collar thickness, Type B should be accepted as an alternative design to Type A (Fig.C.1.11).</u>

KC#989

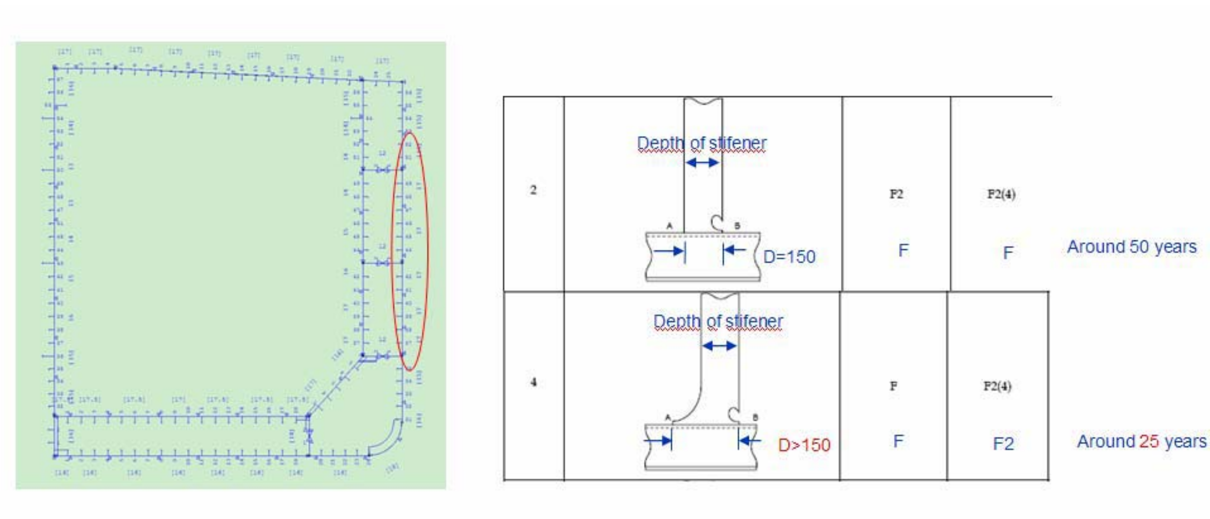

2
Depth of stifener
D=150
F2
F2(4)
F
F
Around 50 years
4
Depth of stifener
D>150
F
F2(4)
F
F2
Around 25 years

KC#996

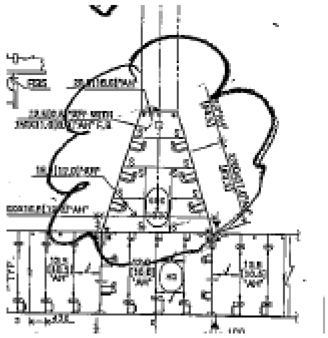

KC#1021 Question

Example of f2 in normal ballast condition for Zone M, stress range combination factor corresponding stress range due to horizontal bending moment

	y/B	f2
UL 1	0.49	0.24
UL 2	0.47	0.22
UL 3	0.46	0.21
UL 4	0.44	0.19

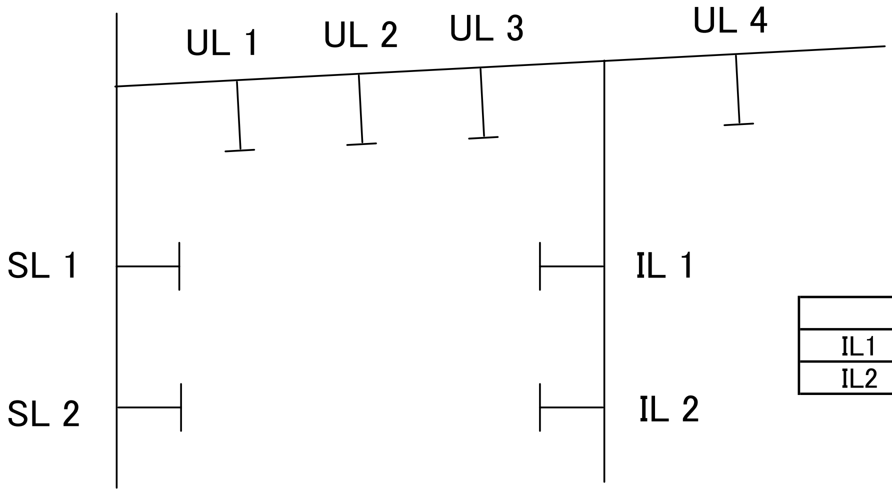

	z/D	f2
SL1	0.97	0.18
SL2	0.94	0.21

	z/D	f2
IL1	0.97	0.49
IL2	0.94	0.47

KC#1021 Answer

Yung S. Shin
e-mail: yshin@eagle.org
American Bureau of Shipping,
Houston, TX 77060, USA

Booki Kim
e-mail: bkim@eagle.org
American Bureau of Shipping,
Houston, TX 77060, USA

Alexander J. Fyfe
e-mail: ajfyfe@pafa.co.uk
PAFA Consulting Engineers, Hampton,
Middlesex, TW12 1BN, UK

Stress Combination for Fatigue Analysis of Ship Structures

A methodology for calculating the correlation factors to combine the long-term dynamic stress components of ship structure from various loads in seas is presented. The proposed methodology is valid for a stationary ergodic narrow-banded Gaussian process. The total combined stress in short-term sea states is expressed by linear summation of the component stresses with the corresponding combination factors. This expression is proven to be mathematically exact when applied to a single random sea. The long-term total stress is similarly expressed by linear summation of component stresses with appropriate combination factors. The stress components considered here are due to wave-induced vertical bending moment, wave-induced horizontal bending moment, external wave pressure, and internal tank pressure. For application, the stress combination factors are calculated for longitudinal stiffeners in midship cargo and ballast tanks of a crude oil tanker. It is found that the combination factors strongly depend on wave heading and period in the short-term sea states. It is also found that the combination factors are not sensitive to the selected probability of exceedance level of the stress in the long-term sense.
[DOI: 10.1115/1.1924399]

Introduction

Ship structures are subjected to various types of loads during voyages. The loads include wave-induced dynamic load, hydrostatic load, transient impact-slamming load, sloshing load, thermal load, and so on. For design, strength evaluation, and fatigue analysis of the ship structures, correlation of the various load-stress components should be properly taken into account. In the design and strength analysis by finite element analysis, the load cases are determined by identifying the dominant load parameters. For each load case, the dominant load response is maximized at a specific wave-heading angle, and the design wave period and height at which the response is at the maximum are determined. Then the load combination factors representing the phase correlation between the dominant load response and secondary load response are determined. This is the so-called regular wave approach, which uses the instantaneous response concept. The load combination factors are basically calculated from transfer functions and phase angles between the dominant and secondary load responses for each load case. This regular wave approach has been widely used in the local scantling and finite element analysis of ship structures [1]. In fatigue analysis of ship structures, however, the long-term stresses rather than instantaneous ones are of main interest. Therefore, an irregular wave approach is more appropriate for combining fatigue load-stress components than the regular wave approach. Various types of load-stress combination methods using the irregular wave approach can be found in [2–6]. In this paper, a consistent and complete method for the combination factors in multiple sea states is presented.

The structural members around fatigue-sensitive locations are subjected to loadings attributed to multiple load effects. Since fatigue is a process of cyclic accumulation of damage in a structure, the cyclic loadings are considered important for fatigue assessment of ship structures. We consider hull girder loads (e.g., vertical and horizontal bendings), external wave pressure, and internal tank pressure resulting from ship motion. These are relatively high-cycle loads that induce the fatigue and occur in a structure in the range of elastic deformation. Other cyclic loadings, such as impact-slamming or low-cycle loads, which may result in significant levels of stress ranges over the expected lifetime of the vessel, are not considered here.

In this paper, we propose a methodology for calculating the stress combination factors, properly accounting for the correlation of the fatigue stress components. The proper combination of stress components is important to derive the total stress values for accurate evaluation of fatigue life. The stress combination factor, in short, represents the relationship between the total stress and each of the stress components. The combination factor should properly take into account the phase correlation between the total stress and each component stress. Here, the total stress at the specific structural location is expressed by linear summation of component stresses with the combination factors. The mathematical formulation is based on an assumption of a stationary ergodic narrow-banded Gaussian process. The formulation can be proven to be mathematically exact when applied to a single random sea. To determine the combination factors in the long-term sense, a generalization procedure for the correlation of extreme values at a given probability of exceedance is necessary. We use the calculated percentage probability of contribution for each scatter diagram entry as a weighting factor to obtain an appropriately weighted value of the combination factors.

For application of the proposed methodology here, the direct calculations of the combination factors are performed for longitudinal stiffeners in midship cargo and ballast tanks of a crude oil tanker. The longitudinals investigated are on the outer bottom, outer side-shell, inner bottom, inner side-shell, deck, and longitudinal bulkhead. The stresses considered here are due to four load components (i.e., wave-induced vertical bending moment, wave-induced horizontal bending moment, external wave pressure, and internal tank pressure). The analysis results show that the combination factors are strongly dependent on wave heading and period in short-term sea states. The combination factors in the long-term sense are also investigated depending on the probability of the exceedance level of the stress value. It is found that the stress combination factors are not dependent on the selected probability level.

Stress Transfer Function

The component stochastic analysis can be used to calculate the stress transfer function at a particular structural location. The transfer function of the stress due to each load component is de-

Contributed by the OOAE Division for publication in the JOURNAL OF OFFSHORE MECHANICS AND ARCTIC ENGINEERING. Manuscript received June 4, 2004. Final manuscript received December 22, 2004. Review conducted by: Chon Tsai.

termined from the load transfer function and stress factor. To calculate the stress transfer function, the corresponding stress factor is multiplied to the load transfer function. The load transfer functions, which are a function of vessel speed, wave heading angle, and wave frequency are the typical outputs of the seakeeping analysis program. The stress factor can be calculated through particular structural analysis techniques, which can be either simple beam theory or finite element analysis procedures. The sophistication of the structural analysis needed depends on the physical system to be analyzed and the type of structural detail and type of structural loading considered. For our application, the stress factors are calculated by the simple beam theory.

The transfer function of the total stress is obtained by simply adding the transfer functions of the component stresses. Therefore, a set of the stress transfer functions can be generated at the vessel speeds, wave headings, and wave frequencies under consideration. The response spectra for the stress transfer functions can then be determined for a given wave spectrum. Summing the stress distributions for the various sea states in the scatter diagram, the long-term distribution of dynamic stresses can be obtained.

Stress Combination Method for a Short-Term Sea State

Consider a one-component stress effect, such as a longitudinal stress in a particular detail. This stress component will receive contributions from several different mechanisms that are based on the response of the overall structure to random waves. We assume contributions arise from four mechanisms, $i=1,2,3,4$, where $i=1$ corresponds to vertical bending, $i=2$ to horizontal bending, $i=3$ to external wave pressure, and $i=4$ to internal tank pressure due to accelerations of fluid in a tank. It is assumed that the stress responses in irregular waves are stationary ergodic narrow-banded Gaussian processes.

Given an input wave spectrum, the relationship between the input spectrum $S_x(\omega)$ and the output (response) spectrum $S_y(\omega)$ for a single component is given by the following equation:

$$S_y(\omega) = H_i(\omega)H_i^*(\omega)S_x(\omega) = |H_i(\omega)|^2 S_x(\omega) \tag{1}$$

where $|H_i(\omega)|$ is the transfer function of the response, e.g., stress transfer function and the superscript * denotes a complex conjugate. The variance (zeroth moment) of a response spectrum is obtained by integrating the spectrum over all encounter frequencies, so obtaining

$$\sigma_c^2 = m_0 = \int_0^\infty S_y(\omega)d\omega = \int_0^\infty |H_i(\omega)|^2 S_x(\omega)d\omega \tag{2}$$

The variance (zeroth moment) of a response spectrum comprising four contributions can be determined according to [6]

$$\sigma_c^2 = m_0 = \int_0^\infty S_y(\omega)d\omega = \sum_{i=1}^{4}\int_0^\infty |H_i(\omega)|^2 S_x(\omega)d\omega + \sum_{i=1}^{4}\sum_{j=1}^{4}{}_{i\neq j}\int_0^\infty H_i(\omega)H_j^*(\omega)S_x(\omega)d\omega \tag{3}$$

Equation (3) can be reexpressed in terms of the variances and correlation coefficients ρ_{ij} of the different contributing components in the form

$$\sigma_c^2 = \sum_{i=1}^{4}\sigma_i^2 + \sum_{i=1}^{4}\sum_{j=1}^{4}{}_{i\neq j}\rho_{ij}\sigma_i\sigma_j \tag{4}$$

where

$$\sigma_i^2 = \int_0^\infty |H_i(\omega)|^2 S_x(\omega)d\omega \tag{5}$$

and

$$\rho_{ij} = \frac{1}{\sigma_i\sigma_j}\int_0^\infty \mathrm{Re}[H_i(\omega)H_j^*(\omega)]S_x(\omega)d\omega \tag{6}$$

Alternatively, ρ_{ij} can be expressed in the form

$$\rho_{ij} = \frac{1}{\sigma_i\sigma_j}\int_0^\infty |H_i(\omega)||H_j(\omega)|(\cos(\phi_j(\omega)-\phi_i(\omega))S_x(\omega)d\omega \tag{7}$$

where ϕ is the phase angle. Writing Eq. (4) explicitly, we have

$$\sigma_c^2 = \sigma_1^2 + \sigma_2^2 + \sigma_3^2 + \sigma_4^2 + 2\rho_{12}\sigma_1\sigma_2 + 2\rho_{13}\sigma_1\sigma_3 + 2\rho_{14}\sigma_1\sigma_4 + 2\rho_{23}\sigma_2\sigma_3 + 2\rho_{24}\sigma_2\sigma_4 + 2\rho_{34}\sigma_3\sigma_4 \tag{8}$$

Alternatively, by generalization of the equations and illustration given in Appendixes A and B, this can be recast as for the combinations of the transfer function in an entirely equivalent form

$$\sigma_c = \rho_{c1}\sigma_1 + \rho_{c2}\sigma_2 + \rho_{c3}\sigma_3 + \rho_{c4}\sigma_4 \tag{9}$$

where ρ_{c1}, ρ_{c2}, ρ_{c3}, and ρ_{c4} are the short-term combination factors. The above results can be generalized to include the direction of ship heading relative to predominant wave direction α and wave-spreading angle μ by using the following expressions:

$$\sigma_i^2(\alpha) = \int_{-\pi/2}^{\pi/2}\int_0^\infty |H_i(\omega,\alpha-\mu)|^2 S_x(\omega,\mu)d\omega d\mu \tag{10}$$

and

$$\rho_{cj}(\alpha) = \int_{-\pi/2}^{\pi/2}\frac{1}{\sigma_c\sigma_j}\int_0^\infty \mathrm{Re}[H_c(\omega,\alpha-\mu) H_j^*(\omega,\alpha-\mu)]S_x(\omega,\mu)d\omega d\mu \tag{11}$$

Since the heading angle is to be represented as uniformly distributed between 0 and 360 deg, the outer integral will be represented as a sum over the specified heading angles divided by number of wave-heading angles considered.

Thus far, the above discussion has been in reference to characteristic values and correlations for response to a single sea state characterized by a given spectrum. This is normally termed as the short-term response. During the course of its design life, the vessel will encounter a large number of spectra with different characteristic values of significant wave height and period and these will be encountered at a range of directions with respect to the vessel's forward speed. The vessel may also be loaded to different levels of draft for significant fractions of its design life.

Stress Combination Method for Long-Term Multiple Sea States

The long-term environment is characterized by a wave scatter diagram that specifies the relative numbers of each sea state that might be experienced over a long period and some rules for the distribution of headings of waves relative to the vessel and the portions of its life in each identified load condition between the waves and the ship. The combined stress associated with a long-term distribution of stress might be calculated from an equation similar in format to that derived for a short-term sea state, namely,

$$\sigma_c^* = C_1\sigma_1^* + C_2\sigma_2^* + C_3\sigma_3^* + C_4\sigma_4^* \tag{12}$$

which is generalized to incorporate four contributing components. Here, σ_c^* is the characteristic value of combined stress at some life-time (probability of exceedance level); σ_1^*, σ_2^*, σ_3^*, and σ_4^* are the characteristic value of the stress component 1 (due to vertical bending), stress component 2 (due to horizontal bending), stress component 3 (external wave pressure), stress component 4 (internal tank pressure), respectively, at the same probability of exceedance level. The long-term correlation coefficients C_1, C_2, C_3, and C_4 are referred to as the stress combination factors for combining long-term responses. For example, C_1 is related to correlation coefficient between combined stress and component 1, and C_2 is related to correlation coefficient between combined stress and component 2. The procedure for determining the combination factors corresponding to a particular probability of exceedance across a combined scatter-diagram-heading distribution of sea states is described below.

For each entry in each scatter diagram for each heading, the zeroth moment of the (short-term) spectral response is determined. Also, we determine the second moment of the (short-term) spectral response, bearing in mind that this value is a function of wave encounter frequency. For the scatter diagram entry associated with each heading, significant wave height and zero-crossing period (of the waves) can be used to calculate the zero-crossing period of the response and hence the number of response cycles. We normalize these values by dividing by the total number of response cycles for all headings and scatter diagram entries.

The contribution that any one scatter-diagram-heading contribution makes to the long-term exceedance distribution of the response is then the sum of Rayleigh distributions multiplied by the normalized number of response cycles, so that the long-term probability that the response will exceed a particular value x is calculated from $\Sigma_k(n_k/n_{\text{total}})p_k \exp(-x^2/2/m_{0k})$, where the sum over k is over the entire set of scatter diagrams of significant wave height, zero-crossing wave period and heading contributions, n_k is the number of stress cycles that will be experienced for each scatter-diagram entry at each heading, n_{total} is the total number of cycles for the entire lifetime summed over all scatter diagram entries and headings, p_k is the probability of occurrence from the wave scatter table, and m_{0k} is the corresponding zeroth moment of the spectral response. The values of x_N that make this expression equal to 10^{-N} are those corresponding to this long-term probability of exceedance

$$\sum_k \frac{n_k}{n_{\text{total}}} p_k \exp\left(-\frac{x_N^2}{2m_{0k}}\right) = \frac{1}{10^N} \tag{13}$$

Once a value of x_N is determined, then substituting this value back into each separate term in the above summation and multiplying by $10^{(N+2)}$ gives the percentage contribution that each scatter-heading entry makes to the 10^{-N} level of exceedance probability. This procedure can be applied to the combined stress or any component stress to determine the relevant component probabilities at any exceedance level for each of the components.

The percentage component probabilities contributing to the combined stress (i.e., the right-hand side of Eq. (12)) have been applied as weighting factors to the calculated correlation coefficients to determine weighted average values of the correlation coefficient that apply to the responses at the specified level of exceedance. That is, the stress combination factor in the long-term sense can be obtained from

$$C_j = \sum_k w_k \rho_{cj}, \quad j = 1,2,3,4 \tag{14}$$

where ρ_{cj} is the stress combination factor in the short-term sense (single seas state); w_k is the weighting factor to derive the stress combination factor in long-term sense, which can be expressed by

$$w_k = 10^N \frac{n_k}{n_{\text{total}}} p_k \exp\left(-\frac{x_N^2}{2m_{0k}}\right) \tag{15}$$

Though not as precise, the alternative expressions for the weighting factor

$$w_k = 10^N p_k \exp\left(-\frac{x_N^2}{2m_{0k}}\right) \tag{16}$$

may be used. It is found that there is no significant difference in the stress combination factors C_j between application of the two weighting methods. This will be discussed further in a following section. Finally, the right-hand side of the postulated Eq. (14) can be evaluated for any exceedance level for each component stress and the weighted averages of the combination factors as specified above.

Table 1 Principal dimensions of 298,000 DWT class crude oil tanker

Length, B. P. (m)	316.0
Length, Scant. (m)	317.69
Breadth, Mld. (m)	60.0
Depth, Mld. (m)	29.7
Draught, Mld. (design) (m)	19.2
Block coeff. (full load)	0.810

Results and Discussions

The stress combination factors have been calculated for longitudinal stiffeners in midship tanks (cargo and ballast tanks) of a 298,300 DWT class crude oil tanker with two different loading conditions (full load and normal ballast). The principal dimensions of the subject vessel are summarized in Table 1.

Figure 1 shows the schematic sketch of the midship section with locations of longitudinal stiffeners for the subject vessel. First, the load transfer functions are obtained by a seakeeping analysis with unit amplitude waves for the combinations of loading conditions, wave headings, and wave frequencies. These calculations are performed using PRECAL [7], a three-dimensional panel code for analyzing the wave-induced motions and loads of the ship in six degrees of freedom. PRECAL has been developed based on linear wave-motion assumptions and a boundary element implementation of three-dimensional forward-speed diffraction-radiation theory. The real and imaginary values of vertical and horizontal bending moments, external wave pressure, and acceleration components at the center of gravity of the tanks are obtained. The load transfer function is then multiplied by the corresponding stress factor to obtain the stress transfer function. The transfer functions of the internal pressure are obtained from the acceleration components of the tank. The vessel speed used is 75% of the design speed, which is 11.25 kn. In present study, the prescribed scatter diagram of significant wave heights and wave periods is the IACS Recommendation No. 34 scatter diagram for trading in the North Atlantic. We use the Pierson-Moskowitz wave spectrum with a cosine-squared spreading function to represent a short-crested wave energy spectrum in the short-term calculations

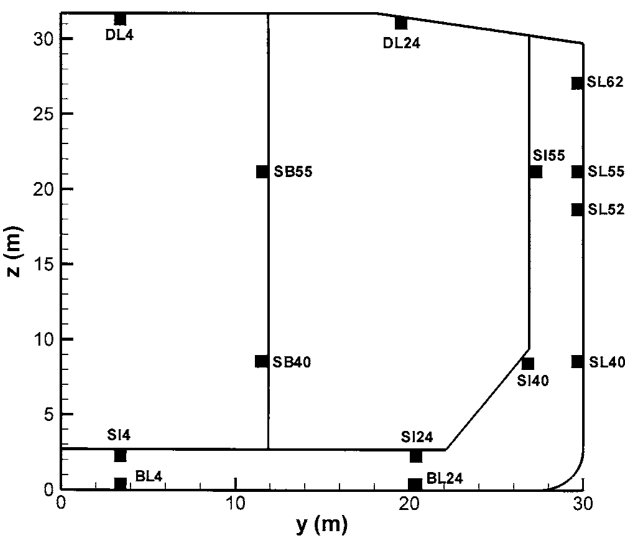

Fig. 1 Sketch of midship section with longitudinal locations for 298,300 DWT crude oil tanker

Table 2 Combination factors and long-term stress values for longitudinal stiffeners in full load condition

Member	σ_{VBM}	C_1	σ_{HBM}	C_2	σ_{PEX}	C_3	σ_{PIN}	C_4	σ_{TOT}
BL4	55.83	0.97	2.58	0.40	10.83	0.60	0	NA	61.86
BL24	55.83	0.87	15.47	0.56	23.26	0.41	0	NA	66.66
SL40	18.27	0.22	22.44	0.78	50.41	0.88	0	NA	65.82
SL52	28.00	0.20	22.49	0.63	56.73	0.93	0	NA	72.59
SL55	39.57	0.32	22.50	0.55	49.85	0.87	0	NA	68.40
SL62	66.56	0.59	22.61	0.31	47.25	0.65	0	NA	77.41
DL4	84.05	1.00	2.58	−0.33	0	NA	0	NA	83.33
DL24	81.16	1.00	14.81	−0.21	0	NA	0	NA	77.77
SI4	47.29	0.98	2.58	0.51	0	NA	18.69	−0.48	38.70
SI24	47.29	0.87	15.47	0.69	0	NA	20.02	−0.32	45.49
SI40	18.88	0.34	20.43	0.86	0	NA	21.20	0.42	32.87
SI55	39.57	0.77	20.85	0.15	0	NA	20.72	0.78	49.85
SB40	18.27	0.82	8.71	0.43	0	NA	14.07	0.52	26.08
SB55	39.57	0.90	8.77	−0.25	0	NA	23.90	0.19	37.83

and equal probability of occurrence of each heading in long-term calculations. Heading of the vessel relative to the waves is assumed to be uniformly distributed between 0 (following seas) and 360 deg with a 30 deg interval.

The stress combination factors and long-term extreme values of stresses at end longitudinal connections for the two different load conditions are obtained from direct calculations, as shown in Tables 2 and 3. All heading contributions are considered in the calculations. The probability of occurrence from the wave scatter table is used as the weighting factor (based on Eq. (16)) to calculate the stress combination factors. As can be seen in the Tables 2 and 3, the combination factors can be much different, even at the same longitudinal location, depending on loading conditions. Here, σ_{VBM}, σ_{HBM}, σ_{PEX}, σ_{PIN}, and σ_{TOT} are the long-term values of stress amplitudes, at the probability level of 10^{-4} due to vertical bending moment, horizontal bending moment, external wave pressure, internal tank pressure, and combined total, respectively. It should be noted that the unit of the stress values is in MPa.

Figure 2 shows the combination factor C_3 related to external wave pressure over wave scatter-diagram entry, i.e., significant wave height $H_{1/3}$ and average zero-crossing wave period T_z. The subject vessel is in ballast condition, the wave heading is 150 deg and the longitudinal SL40 investigated is on the outer-side shell. The results indicate that the combination factor C_3 is independent of the wave height and varies only with the zero-crossing wave period. It is seen in Fig. 3 that the stress combination factor C_3 is a function of wave heading and period. It is found that these observations are also valid for other combination factors C_1, C_2, and C_4.

Figure 4 shows the comparison of the stress combination factor C_1 at the two different probability levels, i.e., 10^{-4} and 10^{-8}. The subject vessel is in full load condition and all wave-heading contributions are considered. The probability of occurrence from the wave scatter table using Eq. (16) is used as the weighting factor. As can be seen in Fig. 4, the combination factors are not much different, depending on the selected probability levels. This observation is valid for all probability levels and similar to the one obtained from a different type of the load combination method as proposed in [8].

The dependence of the combination factor on the different weighting methods is also investigated. The subject vessel is in full load condition, and the probability level is 10^{-4}. The two different weighting methods are used to calculate the combination factor of the extreme value at the given probability of exceedance level; one is based on the number of stress cycles (denoted as "Response" using Eq. (15)), and the other is based on the probability of occurrence from the wave scatter table (denoted as "Wave" using Eq. (16)). As can be seen from the results of the combination factor C_1 in Fig. 5, the combination factors show no significant dependence on the selected weighting method.

Conclusions

A methodology for determining the stress combination factor for the fatigue analysis of ship structures is proposed. The methodology is based on the irregular wave approach that involves the short- and long-term direct calculations. The total stress at the specific structural location is expressed by linear summation of component stresses with the combination factors that consider the phase correlation between the component stress and the total stress. The formulation was mathematically proven to be exact in the short-term sense based on an assumption of a stationary ergodic narrow-banded Gaussian process. A generalization procedure for determining the combination factors of long-term ex-

Table 3 Combination factors and long-term stress values for longitudinal stiffeners in ballast condition

Member	σ_{VBM}	C_1	σ_{HBM}	C_2	σ_{PEX}	C_3	σ_{PIN}	C_4	σ_{TOT}
BL4	51.78	0.95	1.10	0.61	8.13	0.75	20.35	0.84	73.27
BL24	51.78	0.85	6.57	0.57	20.13	0.53	33.16	0.69	81.17
SL40	16.95	0.63	9.53	0.44	29.15	0.55	30.65	0.65	50.80
SL52	25.97	0.15	9.55	−0.02	0	NA	29.57	0.83	28.12
SL55	36.70	0.61	9.55	−0.28	0	NA	26.87	0.39	30.23
SL62	61.73	0.87	9.60	−0.52	0	NA	37.04	0.13	53.40
DL4	77.95	1.00	1.10	−0.65	0	NA	0	NA	77.37
DL24	75.27	1.00	6.29	−0.62	0	NA	0	NA	71.97
SI4	43.86	0.96	1.10	0.63	0	NA	15.10	0.86	55.99
SI24	43.86	0.90	6.57	0.61	0	NA	24.76	0.74	61.78
SI40	17.51	0.77	8.68	0.55	0	NA	26.69	0.80	39.52
SI55	36.70	0.86	8.85	−0.40	0	NA	20.73	−0.01	27.82
SB40	16.95	0.97	3.70	0.73	0	NA	0	NA	19.17
SB55	36.70	1.00	3.72	−0.61	0	NA	0	NA	34.76

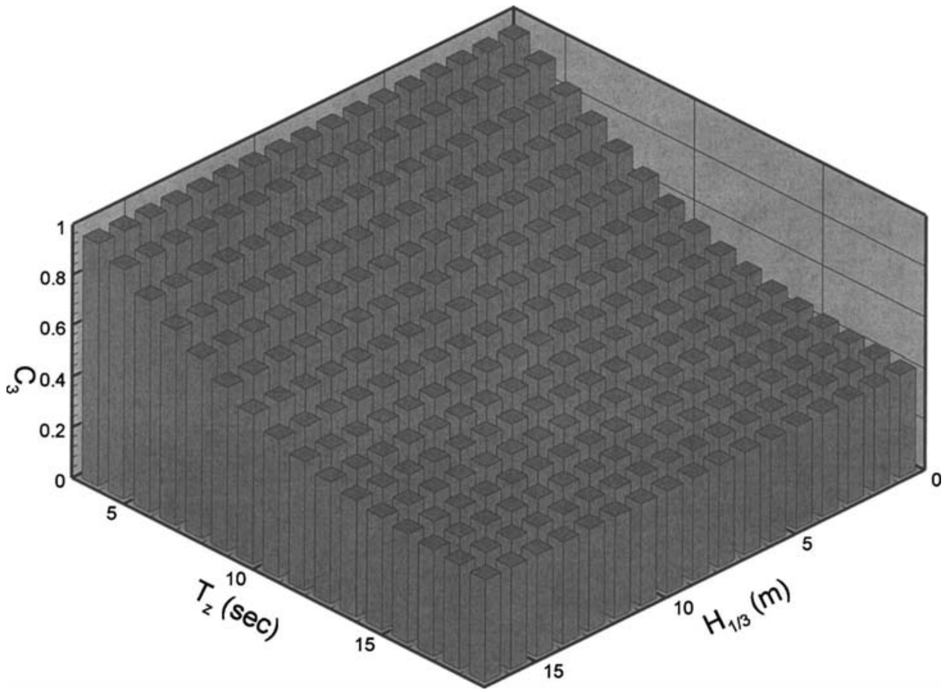

Fig. 2 Combination factor C_3 over wave scatter entry

treme values at the given probability of exceedance level was introduced. It is proposed to use the calculated percentage probability of contribution for each scatter diagram entry as a weighting factor to obtain an appropriately weighted value of the combination factors obtained in short-term sea states.

The direct calculations of the stress combination factors were then performed for end longitudinal connections in midship cargo and ballast tanks of a crude oil tanker in full load and ballast conditions. The results show, in principle, that the combination factors strongly depend on structural location, cargo loading condition, wave heading, and average zero-crossing wave period. It is found that the combination factors for long-term responses in multiple sea states are not sensitive to the selected probability level and the weighting method.

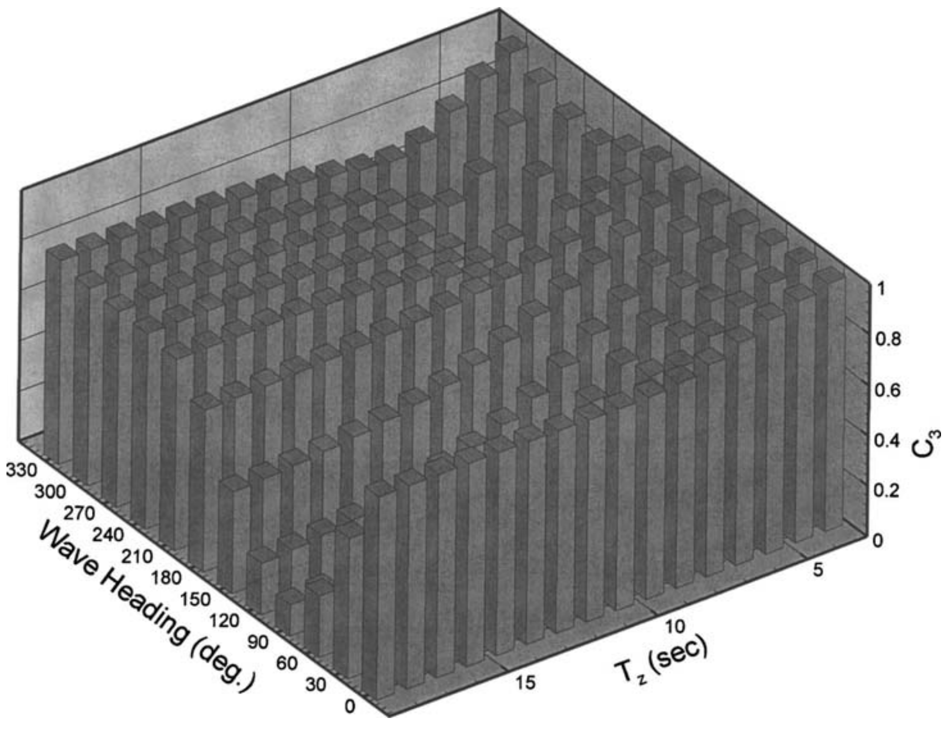

Fig. 3 Combination factor C_3 over wave heading and period

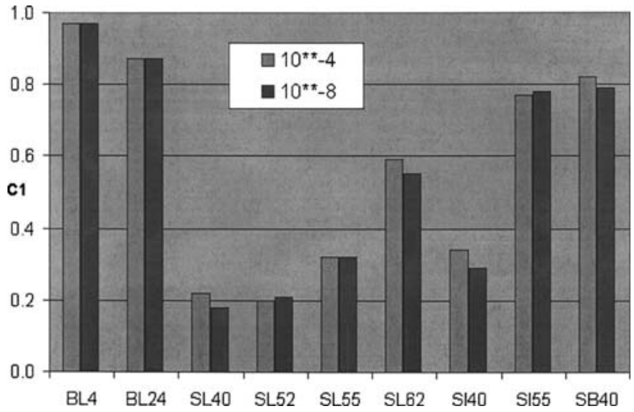

Fig. 4 Combination factor C_1 at probability levels 10^{-4} and 10^{-8}

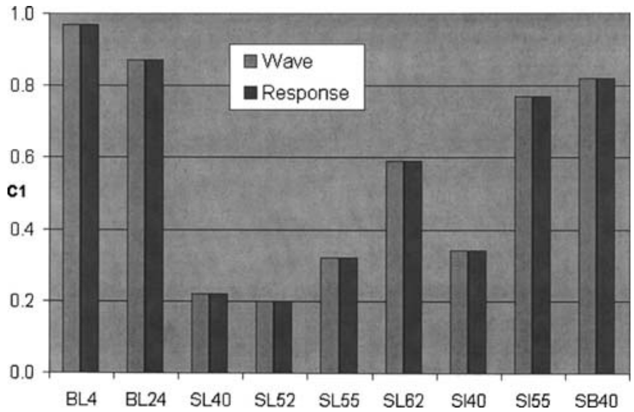

Fig. 5 Combination factor C_1 with different weighting methods

Acknowledgments

The authors would like to thank Dr. Xiaozhi Wang and Dr. Vadim Belenky at American Bureau of Shipping (ABS) for their helpful suggestions and discussions in performing this work.

Appendix A: Equivalence of the Two Expressions for Combination of Transfer Functions

Consider two transfer functions, H_1 and H_2, and the combined transfer function H_c. The accompanying sketch, shown in Fig. 6, and the algebra below demonstrate the equivalence of the two expressions for combining transfer functions. The two expressions are as follows:

$$|H_c|^2 = |H_1|^2 + |H_2|^2 + 2|H_1||H_2|\cos(\phi_2 - \phi_1) \qquad \text{(A1)}$$

which is the normal expression for the third side of a triangle, given two sides and an included angle. If the direction of the resultant is known, an alternative expression is possible

$$|H_c| = |H_1|\cos(\phi_c - \phi_1) + |H_2|\cos(\phi_c - \phi_2) \qquad \text{(A2)}$$

Note that ϕ_c is a function of H_1, H_2, and H_c. Geometrically, the equivalence is intuitively self-evident. The first expression (A1) is the normal result of vector addition obtained according to a "parallelogram" construction, as in parallelogram of forces. The second expression (A2) is visualized as the components of each of the two vectors, H_1 and H_2, resolved along the direction of the resultant. Since these are the only components that can contribute to the resultant, they must sum to the length of the resultant.

To demonstrate equivalence by algebra, express the cosines and sines of the angles involved in terms of the real parts A, the imaginary parts B, and the magnitudes. Then, expand the cosines in the second expression as follows:

$$\cos \phi_1 = A_1/|H_1|, \quad \sin \phi_1 = B_1/|H_1|$$

and similarly for H_2 and H_c

$$|H_c| = |H_1|\{A_c/|H_c| \cdot A_1/|H_1| + B_c/|H_c| \cdot B_1/|H_1|\} + |H_2| \times\{A_c/|H_c| \cdot A_2/|H_2| + B_c/|H_c| \cdot B_2/|H_2|\}$$

$$|H_c|^2 = A_cA_1 + B_cB_1 + A_cA_2 + B_cB_2$$

Substituting $A_c = A_1 + A_2$ and $B_c = B_1 + B_2$, we obtain

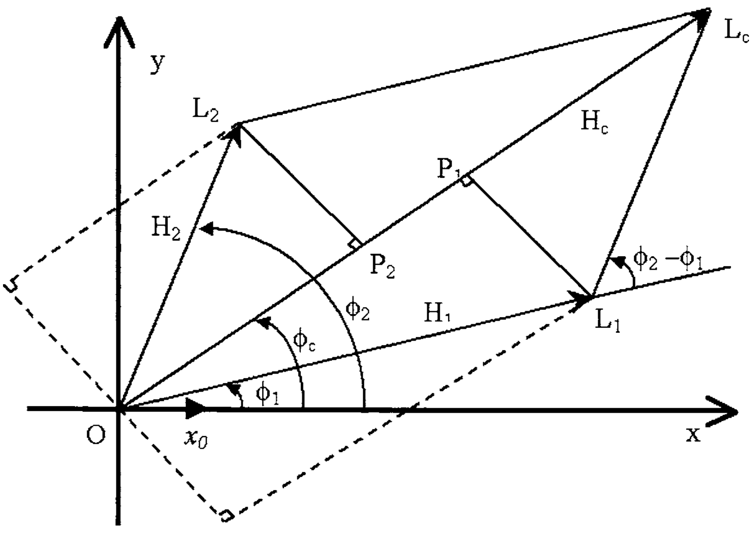

Fig. 6 Sketch for demonstration of equivalence of the two expressions for combining transfer functions

$$|H_c|^2 = |H_1|^2 + |H_2|^2 + 2(A_1A_2 + B_1B_2) = |H_1|^2 + |H_2|^2 + 2|H_1| \times |H_2|\cos(\phi_2 - \phi_1)$$

Similarly, for three components,

$$|H_c|^2 = |H_1|^2 + |H_2|^2 + |H_3|^2 + 2|H_1||H_2|\cos(\phi_2 - \phi_1) + 2|H_1| \times |H_3|\cos(\phi_3 - \phi_1) + 2|H_2||H_3|\cos(\phi_3 - \phi_2)$$

or

$$|H_c| = |H_1|\cos(\phi_c - \phi_1) + |H_2|\cos(\phi_c - \phi_2) + |H_3|\cos(\phi_c - \phi_3)$$

Note that these relationships apply between the transfer functions themselves, and that they are unchanged by multiplication, throughout, by a constant. They apply whether the transfer functions are being used on a deterministic signal to predict the output to a particular input time trace, such as a sinusoid of a particular frequency (in the simplest case), or to a spectral coordinate so that a spectral average value can be obtained.

Because a transfer function is frequency dependent, an identical set of relations will apply at each frequency. For any given spectrum, an average value can be obtained for any or all of the terms on the right-hand side of either equation. Note that it is the application of a spectrum that results in the loss of phase information, not the application of the above equations. Finally, note that each of the cosine terms can be cast as a correlation coefficient. Because in this case it is the common input of a wave train that causes the response, any lack of correlation among inputs or between an input and output signal is due to the phase shift caused by the transfer functions.

Appendix B: Alternative Forms for Combination of Transfer Functions

The equivalence of the two expressions for combining transfer functions can be illustrated with the aid of the vector representation of the transfer functions, as shown in Fig. 6. Here, x_0 represents a unit sinusoidal input, $x_0 \cos \omega t$. H_1 and H_2 represent transfer functions, and H_c is the transfer function obtained by combining H_1 and H_2.

To combine H_1 and H_2 represent them as amplitudes, OL_1, OL_2, and phases, and then either

i. Draw parallelogram $OL_1L_cL_2$, then apply triangle rule in O, L_1, and L_c to give

$$(OL_c)^2 = |H_c|^2 = (OL_1)^2 + (L_1L_c)^2 + (OL_1)(L_1L_c)\cos(\phi_2 - \phi_1)$$

$$|H_c|^2 = |H_1|^2 + |H_2|^2 + |H_1||H_2|\cos(\phi_2 - \phi_1)$$

or

ii. If ϕ_c can be determined, then draw perpendiculars from L_1 and L_2 onto OL_c,

$$OL_c = OP_1 + OP_2$$

$$|H_c| = |H_1|\cos(\phi_c - \phi_1) + |H_2|\cos(\phi_c - \phi_2)$$

References

[1] Liu, D., Spencer, J., Itoh, T., Kawachi, S., and Shigematsu, K., 1992, "Dynamic Load Approach in Tanker Design," Soc. Nav. Archit. Mar. Eng., Trans., **100**, pp. 143–172.

[2] Baarholm, G. S., and Moan, T., 2002, "Efficient Estimation of Extreme Long-Term Stresses by Considering a Combination of Longitudinal Bending Stresses," J. Marine Sci. Technol., **6**(3), pp. 122–134.

[3] Chen, Y. N., and Shin, Y. S., 1997, "Consideration of Loads for Fatigue Assessment of Ship Structures," *Proc. of Workshop and Symposium on the Prevention of Fracture in Ship Structure*, National Research Council, Washington DC.

[4] Funaki, T., Kawabe, H., Hibi, S., Ito, A., Shimizu, H., and Nagata, S., 1996, "A Note on the Correlation Coefficient Between Wave Induced Stress" (in Japanese), J. Soc. Nav. Archit. Japan, **180**, pp. 575–589.

[5] Kawabe, H., Hibi, S., Sasajima, H., and Mikami, K., 1997, "A Note on the Correlation Coefficient Between Wave Induced Stress (2nd Report): Correlation Coefficient of Stresses Between Longitudinal and Lateral Loads" (in Japanese), J. Soc. Nav. Archit. Japan, **182**, pp. 541–549.

[6] Mansour, A. E., 1995, "Extreme Loads and Load Combinations," J. Ship Res., **39**(1), pp. 53–61.

[7] Maritime Research Institute Netherlands, 2002, *PRECAL V5.0 User's Guide*.

[8] Naess, A., 1993, "Statistics of Combined Linear and Quadratic Springing Response of a TLP in Random Waves," *Proc. of 12th International Conference on Offshore Mechanics and Arctic Engineering*, Glasgow, Scotland, **2**, pp. 201–210.

KC#1038

Figure 1.

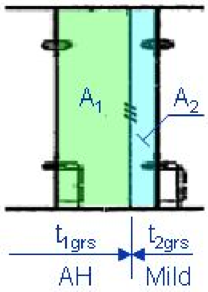

$$t_{FEM\text{-}net50} = \frac{A_1 t_{1grs} + A_2 t_{2grs}}{A_1 + A_2} - 0.5t_{corr}$$